



<http://researchspace.auckland.ac.nz>

ResearchSpace@Auckland

Copyright Statement

The digital copy of this thesis is protected by the Copyright Act 1994 (New Zealand).

This thesis may be consulted by you, provided you comply with the provisions of the Act and the following conditions of use:

- Any use you make of these documents or images must be for research or private study purposes only, and you may not make them available to any other person.
- Authors control the copyright of their thesis. You will recognise the author's right to be identified as the author of this thesis, and due acknowledgement will be made to the author where appropriate.
- You will obtain the author's permission before publishing any material from their thesis.

To request permissions please use the Feedback form on our webpage.

<http://researchspace.auckland.ac.nz/feedback>

General copyright and disclaimer

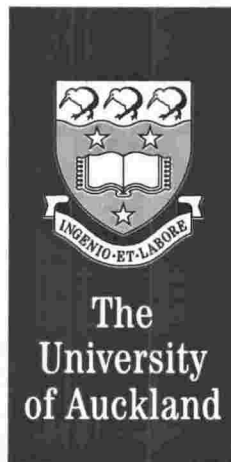
In addition to the above conditions, authors give their consent for the digital copy of their work to be used subject to the conditions specified on the Library Thesis Consent Form.

Machinability Study of Particle Reinforced Aluminium Metal Matrix Composites

by

Richard Jyh-Tsong LIN

The Department of Mechanical Engineering



June, 1998

*A thesis submitted in partial fulfilment of the requirements for the degree of
Doctor of Philosophy in Engineering*

ACKNOWLEDGEMENT

The author would like to express thanks to the following people who have given plentiful of assistance, advice and encouragement towards the completion of this thesis.

Firstly, I am grateful to Professor Debes Bhattacharyya, my supervisor, for his supervision, guidance, support and most important, the timely encouragement throughout the study. His professional knowledge and kind understanding are greatly appreciated. I would also like to thank Associate Professor George Ferguson, from the Department of Chemical and Material Engineering, for his technical advice during the middle stage of the research.

Thanks are due to Comalco Ltd., Australia and Duralcan Ltd, San Diego, USA, especially to Mr. Charles Lane, for the supply of tool inserts, workpiece material as well as technical information.

My sincere thanks go to the technical staff of Solid Mechanics Group, including Terry Boyd, Fred Kwee, Rex Halliwell, Barry Fullerton and Jos Geurts, for their constant help and support. Also thanks are given to Steve O'Brien from the Department of Chemical and Material Engineering for the assistance in metallurgical preparation and microscopy.

The great friendship from the room-mates, Scott Ding, Russell Dykes, Rob Aitken, Carrick Hill, Jeron van Houts, Baden Smith and also all those graduate students who have been involved in the Solid Mechanics Laboratory during the last few years, will always be cherished.

I appreciate the time and effort Mrs. Kate Hyde-Smith and Dr. Martyn Bowis have put in for proofreading parts of my thesis.

Very importantly, I acknowledge the non-stop support from all the families either here or overseas. Without their continuous encouragement and patience, I would not have been here to pursue this cherished goal of my life. Thank you!!

Finally, I would like to dedicate this thesis to my dearest wife, Adela, my most lovely daughter, Olivia and my parents. Thank you for your endless giving.

REVISED ABSTRACT

(For electronic record only)

In this thesis, machinability of particle-reinforced aluminium metal matrix composites, Comral-85 and *DURALCAN*TM, has been studied. Continuous turning of round composite bars, using polycrystalline diamond (PCD) inserts has been selected as the test method. The test conditions included cutting speeds varying from 75 to 700m/min and feed rates from 0.1 to 0.4 mm/rev with constant depth of cut of 0.5 mm.

The main wear mechanism of machining these Al MMC materials is abrasion by the reinforcing particles and the primary type of tool wear is flank wear. Linear regression techniques has been used to derive Taylor equations to describe the tool performance. The results show that the time required to reach the tool wear limit decreases with increased speed and feed rate. However, the volume of material removed before reaching the wear limit actually increases with the higher feed rate. This apparent anomaly has been reconciled in a modified Taylor equation.

As for surface finish, the feed rate is found to be a more dominant factor than cutting speed. The higher the feed rate is, the worse the surface finish becomes. The surface finish is found to improve with tool wear at early stage because of the increase of tool nose radius; after that it starts deteriorating as a consequence of excessive tool wear.

The change of feed rate is also more influential on the variation of machining forces than that of cutting speed. Using the same regression techniques, the general machining force-tool wear equations are derived. The results show that the equation derived from the feed force is better suited to monitor tool wear than that derived from the cutting force. The general relationship between tool wear and power consumption has also been established.

The chip forming mechanism while machining *DURALCAN*TM MMC has also been studied by using an explosive charged "quick-stop" device. The primary chip forming mechanism involves the initiation of cracks due to the high shear stress, followed by the decohesion of particles and matrix material within the chip due to the stress concentration on the edge of the particles. The crack propagation is enhanced through the microvoid coalescence within matrix material. The fracture and the sliding of material then follow to form semi-continuous "saw-toothed" chips.

ABSTRACT

With the increasing usage of metal matrix composites (MMCs) in various applications such as aerospace, automotive and sports related industries, the machining of such materials has become a very important subject to study. Owing to the addition of reinforcing materials which are normally harder and stiffer, the machining becomes significantly more difficult than that of conventional monolithic materials. Among many types of MMCs, the most popular types are aluminium alloys reinforced with ceramic particles since they cost less but provide favourable properties with only a minimum increase in density over the base alloy. These properties include high specific strength/stiffness, wear and corrosion resistance and fatigue resistance, etc.. In this thesis, machinability of particle-reinforced aluminium metal matrix composites has been studied.

Continuous turning of round composite bars, made from Comral-85 and *DURALCAN*TM, using polycrystalline diamond (PCD) inserts, with average diamond size of 25- μ m, has been selected as the test method. The test conditions included cutting speeds varying from 75 to 700m/min and feed rates from 0.1 to 0.4 mm/rev while the depth of cut was kept constant at 0.5 mm. The four machinability related aspects, namely tool wear, surface finish, machining forces and power consumption, are constantly monitored during the machining process. The nature of chips formed is also recorded for further analysis.

It has been confirmed that the main wear mechanism of machining particulate reinforced aluminium MMC materials is abrasion by the reinforcing particles and the primary type of tool wear is flank wear. The performance of the tools is, therefore, based on the development of flank wear, which has been monitored by optical and scanning electron microscopy. The tool life criterion for machining Comral-85 is 0.3-mm flank wear, whereas for machining of *DURALCAN*TM composite, the tool life criterion is up to flank wear of 0.25 mm. The tool life data have been analysed using linear regression techniques and a traditional Taylor model involving cutting speed only has been established for this material. A general form of the Taylor equation has also been developed by regression methods to describe the tool performance. The results show that the time required to reach the tool wear limit decreases with increased speed and feed rate. However, the volume of material removed before reaching the wear limit actually

increases with the higher feed rate. This apparent anomaly has been reconciled by rewriting the Taylor equation in a modified form.

In the aspect of surface finish, it has been found that the feed rate is a more dominant factor than cutting speed. The higher the feed rate is, the worse the surface finish becomes. Therefore, in the selection of machining parameters, after taking into account of the surface finish allowed, the feed rate should be as high as possible to achieve the maximum material volume removal. On the other hand, the change of surface roughness while machining at a constant speed is mainly due to the progress of tool wear. The surface finish is found to improve with tool wear before the flank wear reaches around 0.15 mm because of the rounding of tool nose radius; after that it starts deteriorating as a consequence of excessive tool wear.

Similar to surface finish, the change of feed rate is more influential on the variation of machining forces than that of cutting speed. Nevertheless, the change of cutting speed has a resembling effect on machining forces as that on the growth of tool wear. Consequently, the recorded machining force data against tool wear have also been analysed using the same regression techniques to derive the general machining force-tool wear equations. The derived tool wear-machining force equation can be used to indirectly monitor the development of tool wear during machining operation for deciding the tool life. The results show that the equation derived from the feed force data is better suited to monitor tool wear than the one derived from the cutting force.

As the result of the direct relationship between cutting force and power consumption, the power consumption data have also been regressively analysed. The general relationship between tool wear and power consumption has been established. Even though this relationship is a more conservative approach, it can be the other way of indirectly monitoring the tool wear growth with sufficient accuracy.

Lastly, the chip forming mechanism while machining *DURALCAN*TM composite material has also been studied by using an explosive charged “quick-stop” device. During the chip breaking process, the primary chip forming mechanism involves the initiation of cracks from the outer free surface of the chip due to the high shear stress. Meanwhile, some small voids are formed by the decohesion of particles and matrix material within the chip due to the stress concentration on the edge of the particles. The crack propagation is enhanced through the microvoid coalescence

within matrix material from one particle to the other along the shear plane. The fracture and the sliding of material then follow to form semi-continuous "saw-toothed" chips. The average shear angle has been found to increase slightly with the increasing cutting speed, hence, thinner chips are formed and easily broken into smaller pieces with higher cutting speeds. However, for the formation of "saw-toothed" chip, the shear angle varies during chip forming and the variation is more significant with the increasing cutting speed.

Table of Contents

Acknowledgement	ii
Abstract	iii
Table of Contents	vi
List of Figures	x
List of Tables	xvi
List of Appendices	xvii
CHAPTER 1 INTRODUCTION	1
1-1 Composite Materials	1
1-2 Metal Matrix Composites (MMCs)	2
1-3 Machining of MMCs	3
1-4 Outline of Thesis	5
CHAPTER 2 LITERATURE SURVEY	7
2-1 Aluminium Metal Matrix Composites	7
2-1.1 Matrix	7
2-1.2 Reinforcements	8
2-1.2.1 Forms of Reinforcements	8
2-1.2.2 Types of Reinforcements	8
2-1.3 SiC Reinforced Aluminium MMCs	9
2-1.4 Al ₂ O ₃ microsphere reinforced Aluminium MMC	9
2-2 Machining of Aluminium Metal Matrix Composites	9
2-2.1 Machining Aluminium MMCs with carbide or other tool materials	11
2-2.1.1 Turning	11
2-2.1.2 Milling	13
2-2.1.3 Drilling	13
2-2.1.4 Other Operations	15
2-2.2 Machining Aluminium MMCs with Polycrystalline Diamond Tools	15
2-2.2.1 Turning	17
2-2.2.2 Milling	18

2-2.2.3	<i>Drilling</i>	19
2-2.2.4	<i>Other Operations</i>	20
2-2.3	<i>Assessment of Machinability</i>	20
2-2.3.1	<i>Tool Life</i>	22
2-2.3.2	<i>Surface Finish</i>	23
2-2.3.3	<i>Machining Forces</i>	25
2-2.3.4	<i>Chip Formation</i>	26
2-2.4	<i>Machining aluminium MMCs with Coolant</i>	27
2-2.5	<i>Machining with Diamond-Coated Tools</i>	28
2-3	<i>Objectives of Current Research</i>	29

CHAPTER 3 EXPERIMENTAL PROCEDURES 42

3-1	<i>Materials</i>	42
3-2	<i>Experimental Set-Up</i>	45
3-3	<i>Polycrystalline Diamond Tools</i>	48
3-4	<i>Diamond-Coated Tools</i>	50
3-5	<i>Quick-Stop Device</i>	51

CHAPTER 4 MACHINING OF COMRAL-85 AND DURALCAN MMCS : RESULTS AND DISCUSSION 53

4-1	<i>Machining aluminium MMCs with PCD tools</i>	53
4-1.1	<i>Machining of the Comral-85 material (cutting speed < 300 m/min)</i>	53
4-1.1.1	<i>Tool Wear</i>	55
4-1.1.2	<i>Surface Finish</i>	57
4-1.1.3	<i>Machining Forces</i>	59
4-1.1.4	<i>Cutting Power</i>	61
4-1.2	<i>Machining of the DURALCANTM material (cutting speed ≥ 300 m/min)</i>	63
4-1.2.1	<i>Tool Wear</i>	64
4-1.2.2	<i>Surface Finish</i>	65
4-1.2.3	<i>Machining Forces</i>	70
4-1.2.4	<i>Cutting Power</i>	75
4-1.3	<i>Discussion</i>	78

4-1.3.1	<i>Tool Wear</i>	78
4-1.3.2	<i>Surface Finish</i>	79
4-1.3.3	<i>Machining Forces & Cutting Power</i>	81
4-2	<i>Effects of Using Cutting Fluid</i>	84
4-2.1	<i>Tool Wear and Tool Life</i>	85
4-2.2	<i>Surface Finish</i>	89
4-2.3	<i>Machining Forces</i>	91
4-2.4	<i>Cutting Power</i>	94
4-3	<i>Machining DURALCAN MMC Material with Diamond Coated Tool</i>	96
4-3.1	<i>Tool Wear and Tool Life</i>	97
4-3.2	<i>Surface Finish</i>	101
CHAPTER 5	STATISTICAL MODELING OF TOOL PERFORMANCE	103
5-1	<i>Tool Life</i>	103
5-1.1	<i>Machining Comral-85 MMC</i>	103
5-1.2	<i>Machining DURALCANTM MMC</i>	106
5-1.2.1	<i>Tool Life in Terms of Time</i>	106
5-1.2.2	<i>Tool Life in Terms of Material Removal</i>	108
5-2	<i>Wear-Machining Force Relationships</i>	112
5-3	<i>Wear-Cutting Power Relationship</i>	120
CHAPTER 6	CHIP FORMATION MECHANISM OF MACHINING ALUMINIUM METAL MATRIX COMPOSITE	126
6-1	<i>Chip Samples Examination</i>	126
6-2	<i>Chip Forming Mechanism</i>	128
6-2.1	<i>Chip Formation</i>	130
6-2.2	<i>Shear Angle Relationship with Cutting Speed</i>	137
6-2.3	<i>Built-up Edge of Chip Formation</i>	139

CHAPTER 7	CONCLUDING REMARKS, ACCOMPLISHMENTS & RECOMMENDATIONS	141
7-1	<i>Concluding Remarks</i>	141
7-2	<i>Accomplishments</i>	145
7-2	<i>Recommendations for Future Works</i>	146
REFERENCES		147
BIBLIOGRAPHY		152
APPENDICES		A-1

List of Figures

Figure 3-1	Microstructure of alumina-containing MICRAL-20R microsphere reinforced Comral-85 aluminium matrix composite.	43
Figure 3-2	Microstructure of <i>DURALCAN</i> TM aluminium matrix composite.	44
Figure 3-3	Material Properties for Comral-85 at Elevated Temperatures.	46
Figure 3-4	The machine set-up for this research.	47
Figure 3-4.1	The tool insert and tool holder. (circled in Fig 3.4)	48
Figure 3-5	Criteria based on features of tool flank wear [5].	48
Figure 3-6	The Surtronic-3 Talysurf surface roughness measurer.	49
Figure 3-7	The PCD tool inserts used in this research.	49
Figure 3-8	The diamond-coated tool inserts used in this research.	50
Figure 3-9	The explosive quick-stop device.	51
Figure 3-10	Constructional details of the explosive quick-stop device.	52
Figure 4-1	The tool wear growth curves when machining Comral-85. ($f = 0.16$ mm/rev, $d = 0.5$ mm)	55
Figure 4-2	The tool wear growth curves when machining Comral-85 at three different speeds. ($f = 0.16$ mm/rev, $d = 0.5$ mm)	56
Figure 4-3	The typical wear growth on the flank surface of the PCD insert while machining Comral-85 material.	56
Figure 4-4	The recorded surface profiles of the machined surfaces at three different speeds. ($f = 0.16$ mm/rev, $d = 0.5$ mm)	57
Figure 4-5	The variation of surface roughness when machining Comral-85 at three different speeds. ($f = 0.16$ mm/rev, $d = 0.5$ mm)	58
Figure 4-6	The variation of surface roughness against tool wear when machining Comral-85 at three different speeds. ($f = 0.16$ mm/rev, $d = 0.5$ mm)	58
Figure 4-7	The variation of machining forces when machining Comral-85 at three different speeds (F_x : feed force; F_z : cutting force). ($f = 0.16$ mm/rev, $d = 0.5$ mm)	59
Figure 4-8	The variation of machining forces verse tool wear when machining Comral-85 at three different speeds (F_x : feed force; F_z : cutting force). ($f = 0.16$ mm/rev, $d = 0.5$ mm)	60

Figure 4-9	The plotted record of machining forces used for force measurement shows the fluctuation of both cutting and feed forces during the machining process. (100 N/Div for Force axis and 1 Sec/Div for Time axis)	60
Figure 4-10	The variation of power needed when machining Comral-85 at three different speeds. ($f = 0.16$ mm/rev, $d = 0.5$ mm)	61
Figure 4-11	The variation of power verse tool wear when machining Comral-85 at three different speeds. ($f = 0.16$ mm/rev, $d = 0.5$ mm)	62
Figure 4-12	The typical wear growth on the flank surface of the PCD insert while machining <i>DURALCAN</i> material.	64
Figure 4-13	The tool wear growth curves when machining <i>DURALCAN</i> at three different speeds with constant feed rate. ($d = 0.5$ mm)	66
Figure 4-14	The tool wear growth curves when machining <i>DURALCAN</i> at three different feed rates with constant cutting speed. ($d = 0.5$ mm)	67
Figure 4-15	The recorded surface profile of the machined surface for <i>DURALCAN</i> material at three different cutting conditions. ($d = 0.5$ mm)	68
Figure 4-16	The variation of surface roughness when machining <i>DURALCAN</i> at three different speeds with constant feed rate. ($d = 0.5$ mm)	69
Figure 4-17	The variation of surface roughness when machining <i>DURALCAN</i> at three different feed rates with constant cutting speed. ($d = 0.5$ mm)	71
Figure 4-18	The variation of machining forces when machining <i>DURALCAN</i> at three different speeds with constant feed rate (F_x : feed force; F_z : cutting force). ($d = 0.5$ mm)	72
Figure 4-19	The variation of machining forces against tool wear when machining <i>DURALCAN</i> at three different speeds with constant feed rate (F_x : feed force; F_z : cutting force). ($d = 0.5$ mm)	73
Figure 4-20	The variation of machining forces when machining <i>DURALCAN</i> at three different feed rate with constant cutting speed (F_x : feed force; F_z : cutting force). ($d = 0.5$ mm)	74
Figure 4-21	The variation of power consumption when machining <i>DURALCAN</i> at three different speeds with constant feed rate. ($d = 0.5$ mm)	76
Figure 4-22	The variation of power consumption when machining <i>DURALCAN</i> at three different feed rate with constant cutting speed. ($d = 0.5$ mm)	77

Figure 4-23	The SEM picture of wear land on the tip of PCD tool (Arrows indicate the directions of movement of workpiece material relative to the tool surfaces).	78
Figure 4-24	The variation of surface roughness against tool wear when machining <i>DURALCAN</i> at three different speeds with the same feed rate. ($d = 0.5$ mm)	79
Figure 4-25	Effect of cutting speed on surface finish.	80
Figure 4-26	Composite cutting force circle.	82
Figure 4-27	The cutting trace of an advancing tool.	83
Figure 4-28	The top rake surface around nose radius of the PCD tool insert before and after machining <i>DURALCAN</i> material in wet condition.	86
Figure 4-29	The worn flank surface of the PCD insert for machining <i>DURALCAN</i> with cutting fluid at 700 m/min and 0.4 mm/rev.	86
Figure 4-30	The comparison of tool wear growth curves when machining <i>DURALCAN</i> with and without cutting fluid at three different feed rates with constant cutting speed of 700 m/min. ($d = 0.5$ mm)	88
Figure 4-31	The comparison of tool wear growth curves when machining <i>DURALCAN</i> with and without cutting fluid at two different cutting speeds with constant feed rate of 0.4 mm/rev. ($d = 0.5$ mm)	88
Figure 4-32	The chip travelling mark on the tool rake surface. (The white strip in between the two dotted lines is the chip travelling mark.)	89
Figure 4-33	The comparison of surface finish when machining <i>DURALCAN</i> with and without cutting fluid at three different feed rates with constant cutting speed of 700 m/min. ($d = 0.5$ mm)	90
Figure 4-34	The comparison of surface finish when machining <i>DURALCAN</i> with and without cutting fluid at two different cutting speeds with constant feed rate of 0.4 mm/rev. ($d = 0.5$ mm)	90
Figure 4-35	The machined surface profiles when machining the <i>DURALCAN</i> MMC with and without cutting fluid.	91
Figure 4-36	The comparison of feed force when machining <i>DURALCAN</i> with and without cutting fluid at three different feed rates with constant cutting speed of 700 m/min. ($d = 0.5$ mm)	92
Figure 4-37	The comparison of feed force when machining <i>DURALCAN</i> with and without cutting fluid at two different cutting speeds with constant feed rate of 0.4 mm/rev. ($d = 0.5$ mm)	92

Figure 4-38	The comparison of cutting force when machining <i>DURALCAN</i> with and without cutting fluid at three different feed rates with constant cutting speed of 700 m/min. ($d = 0.5$ mm)	93
Figure 4-39	The comparison of cutting force when machining <i>DURALCAN</i> with and without cutting fluid at two different cutting speeds with constant feed rate of 0.4 mm/rev. ($d = 0.5$ mm)	93
Figure 4-40	The comparison of power consumption when machining <i>DURALCAN</i> with and without cutting fluid at three different feed rates with constant cutting speed of 700 m/min. ($d = 0.5$ mm)	95
Figure 4-41	The comparison of power consumption when machining <i>DURALCAN</i> with and without cutting fluid at two different cutting speeds with constant feed rate of 0.4 mm/rev. ($d = 0.5$ mm)	95
Figure 4-42	The flank wear and the damaged cutting edge of the diamond coated inserts at three different cutting conditions.	99
Figure 4-43	The failure of the diamond-coated TPG 322 insert when machining <i>DURALCAN</i> material at 500 m/min and 0.2 mm/rev.	100
Figure 4-44	The machined surface of the <i>DURALCAN</i> material by using the diamond-coated inserts.	101
Figure 5-1	Tool life against cutting speed for machining Comral-85 MMC material; (a) Normal scale and (b) Double log scale.	105
Figure 5-2	The comparison of experimental tool life with the value from the Taylor equation for increasing cutting speed, in terms of (a) time and (b) material removal.	109
Figure 5-3	The comparison of experimental tool life with the value from the Taylor equation for increasing feed rate, in terms of (a) time and (b) material removal.	110
Figure 5-4	The typical wear curve in three different cutting conditions.	113
Figure 5-5	The recording of machining forces versus time in three different cutting conditions; (a) Feed force and (b) Cutting force.	114
Figure 5-6	Regression results of the tool wear against feed force; (a) 300 m/min, 0.1 mm/rev and (b) 700 m/min, 0.4 mm/rev.	115
Figure 5-7	Regression results of the tool wear against cutting force; (a) 300 m/min, 0.1 mm/rev and (b) 700 m/min, 0.4 mm/rev.	116

Figure 5-8	General regression results of the tool wear against feed force (compared with experimental data); (a) 300 m/min and 0.1 mm/rev and (b) 700 m/min and 0.4 mm/rev.	118
Figure 5-9	General regression results of the tool wear against cutting force (compared with experimental data); (a) 300 m/min and 0.1 mm/rev and (b) 700 m/min and 0.4 mm/rev.	119
Figure 5-10	Power consumption against tool wear for machining <i>DURALCAN</i> MMC at three different conditions.	120
Figure 5-11	Regression results of the tool wear against power consumption; (a) 300 m/min, 0.1 mm/rev and (b) 700 m/min, 0.4 mm/rev.	122
Figure 5-12	General regression results of the tool wear against power consumption (compared with experimental data); (a) 300 m/min and 0.1 mm/rev and (b) 700 m/min and 0.4 mm/rev.	124
Figure 5-13	Comparison of the regressional results for the power-wear relationship directly from power reading (Solid) and transformed from cutting force-wear relationship (Dotted); (a) 300 m/min, 0.1 mm/rev and (b) 700 m/min, 0.4 mm/rev.	125
Figure 6-1	The changes of chip types during machining Comral-85.	127
Figure 6-2	Change of chip type during machining <i>DURALCAN</i> material.	127
Figure 6-3	The two typical chips formed during machining <i>DURALCAN</i> composite material, (a) long washer helical type; (b) loose arc chips.	128
Figure 6-4	The two basic models for metal cutting analysis.	129
Figure 6-5	The photos of the chip formed during machining SiC reinforced MMC in three different cutting speeds; (a) 300 m/min, (b) 500 m/min and (c) 700 m/min.	131
Figure 6-6	Models of chip formation [67].	132
Figure 6-7	The semi-continuous type of chips formed during machining <i>DURALCAN</i> material.	132
Figure 6-8	The microstructures of the chip root.	133
Figure 6-9	The separation of particles and the matrix material within the chip.	133
Figure 6-10	(a) Shear fracture of the chip formed, (b) Higher magnification of (a) to show the shear marks of the fractured material.	134
Figure 6-11	Different stages of crack propagation; crack propagates (a) through, (b) nearly through and (c) about half way through the chip thickness.	135

Figure 6-12	The morphology of the side flow material.	136
Figure 6-13	The “stick-slip” marks on the smooth side of chip.	136
Figure 6-14	The fluctuation of the forces measurement during machining. (100 N/Div for Force axis and 1 Sec/Div for Time axis)	137
Figure 6-15	The microstructures at the vicinity of the chip root.	139

List of Tables

Table 2-I	Comparison of the suitability of different tool materials [21].	21
Table 2-II	A summary of reference materials.	30
Table 3-I	Chemical composition of COMRAL-85 material (wt%).	43
Table 3-II	Chemical composition of <i>DURALCAN</i> F3S.20P material (wt%).	44
Table 3-III	Tensile properties of Comral-85, <i>DURALCAN</i> aluminium MMCs and their matrix materials.	45
Table 3-IV	High temperature tensile properties for <i>DURALCAN</i> aluminium MMC. (Typical values for two soak times)	46
Table 3-V	Properties of polycrystalline diamond compared with the other tool materials. [17,22]	50
Table 4-I	Summary of experimental conditions for machining Comral-85 material.	54
Table 4-II	Summary of experimental conditions for machining <i>DURALCAN</i> material.	64
Table 4-III	Summary of experimental conditions for machining <i>DURALCAN</i> material with cutting fluid.	85
Table 4-IV	Comparison of tool lives for the dry and wet cutting conditions.	89
Table 4-V	Summary of experimental conditions for machining <i>DURALCAN</i> material with diamond-coated tools.	98
Table 5-I	The tool life of PCD insert for machining Comral-85 at three different cutting speed.	104
Table 5-II	The experimental results used in regression analysis and the regression result.	107
Table 6-I	Experimental details for chip forming analysis.	130
Table 6-II	Values of the average shear angles for the three different speeds.	138

List of Appendices

Appendix A-A	Comalco Data Sheet	A-2
Appendix A-B	Duralcan Data Sheets	A-3
Appendix B	Explanation of the tool code for PCD insert (TPG xxx)	A-6
Appendix C	Mechanical, physical, and thermal properties of PCD, PCBN, and other materials [22]	A-7
Appendix D	Typical machining parameters for PCD tooling [22]	A-8
Appendix E	Description of cutting fluid, HOCUT 757	A-9
Appendix F	The Rest of Regression Results	A-10
Appendix G	The Characteristics of Chip Forms	A-15
Appendix H	List of Publications	A-16